Positron Annihilation in an Interacting Electron Gas*

J. P. CARBOTTE† AND S. KAHANA
Physics Department, McGill University, Montreal, Canada
(Received 3 February 1965)

The effects of self-energy, as well as hole-particle interaction processes, on the angular correlation of gamma rays from positrons annihilating in an electron gas are studied. The two regions corresponding to emission of momentum smaller and greater than the Fermi momentum p_F are discussed separately. In the first instance, it is found that self-energy effects, at least in the high-density limit, can be accounted for adequately simply by using the static approximation to the dynamic potential in the first-order ladder graph and ignoring altogether first-order self-energy corrections, provided, of course, a plasmon correction is made. In the second case it is shown that owing to dynamic polarization effects the tails occurring beyond p_F are not at all comparable to those expected on a simple model where the positron force is ignored but correlations within the electron gas are treated properly. Hole-particle interaction graphs are not important since they occur in pairs which cancel each other.

I. INTRODUCTION

In a recent paper[1] one of the present authors discussed a theory of positron annihilation in an electron gas which led to rates in good agreement with experiment. The approach to the many-particle system used in K-II was a zero-temperature Green's-function technique.[2,3] In this formalism the annihilation rate is given as a simple quadrature of an appropriate contraction of the electron-positron Green's function. By summing the set of all ladder graphs in the perturbation series for this correlation function, it can be shown that the contribution to the total annihilation rate from an electron in a state of momentum $\mathbf{p}$ (with p smaller than the Fermi momentum p_F) is not simply proportional to 1, as expected on a Sommerfeld model, but must be multiplied by an enhancement factor $\epsilon(\mathbf{p})$. To get reasonable enhancement factors one must, of course, include carefully in the calculation the polarization of the background electron gas by the annihilating pair. The physical meaning of $\epsilon(\mathbf{p})$ is simple. It is given by the square of a Bethe-Goldstone-type amplitude $\psi_p(\mathbf{x}_e;\mathbf{x}_p)$ evaluated at $\mathbf{x}_e=\mathbf{x}_p$ where $\mathbf{x}_e(\mathbf{x}_p)$ is the electron (positron) coordinate. This amplitude can be interpreted as the wave function of an electron-positron pair interacting through a suitable screened Coulomb force and immersed in a quiescent Fermi sea. The uncorrelated part of $\psi_p(\mathbf{x}_e;\mathbf{x}_p)$ describes a free electron of momentum $\mathbf{p}$ and a positron at rest, while the coherent part accounts for the electron-positron coupling.

The enhancement factors arrived at in this way are quite large. For instance, in sodium they are of the order of 13. This demonstrates well that the positron Coulomb field is very important in the present context. In view of this, one may well wonder whether the success of the theory given in K-II is not to some extent fortuitous since many diagrams in the expansion of the electron-positron correlation function involving positron-electron interaction lines were somewhat arbitrarily ignored. Further the work in K-II is concerned only with annihilation resulting in the emission of two quanta of momentum $\mathbf{p}$ with $p<p_F$. It needs to be extended to the region $p>p_F$.

The principal aim of this paper is twofold. First, we would like to estimate, at least in the lower orders of the perturbation series, all graphs involving an electron-positron interaction line. Only then can we be reasonably certain that the theory of K-II gives an adequate description of the disturbance of the electronic configuration introduced by the positron probe. Secondly, we would like to understand how the self-energy processes are to be fitted into the general calculation.

In Sec. II the high-density limit of the theory given in K-II is re-examined and corrected. For momentum $p<p_F$ an enhancement factor $\epsilon^{\text{h.d.}}(\mathbf{p})$ is defined and its variation as a function of $\mathbf{p}$ is studied. How electron and positron first-order self-energy corrections affect this enhancement factor is the subject of Sec. III. An attempt at extending the discussion to include self-energy processes in higher order ladder graphs would immediately involve us in relatively complicated second-order diagrams having a self-energy part with a further electron-positron ladder step. It is convenient to leave such considerations to Sec. VI and to turn instead to a study of the simpler second-order processes, namely, the two hole-particle interaction diagrams. These are discussed in Sec. IV.

The task of Sec. V is to investigate the contribution to the partial annihilation rate, with emission of momentum $p>p_F$, from each of the five processes previously studied in the case $p<p_F$. In this section some speculations on the effect of higher order pure self-energy diagrams are also included. In Sec. VI we generalize the work of V to include enhancement

* Based on part of a Ph. D. thesis submitted by J. P. Carbotte to the Graduate Faculty of McGill University. This author would like to express his gratitude to the National Research Council of Canada for support during 1962 and 1963 in the form of a Studentship. Financial aid for publication from the National Research Council is also gratefully acknowledged.

† Present address: Laboratory of Atomic and Solid State Physics, Cornell University, Ithaca, New York.

[1] S. Kahana, Phys. Rev. **129**, 1622 (1963). Referred to from here on as K-II.

[2] A. Klein and R. E. Prange, Phys. Rev. **112**, 904 and 1008 (1958).

[3] A. Klein, *Lectures on the Many-Body Problem*, edited by E. R. Caianiello (Academic Press Inc., London, 1962), p. 279.

factors. This problem is of course intimately connected with that of extending the theory of Secs. II and III ($p<p_F$) to higher order ladder graphs. The analogy between the two situations is very suggestive. However, we have made no detailed calculation in this latter case. Finally, in Sec. VII the more important results obtained are summarized and a number of remarks are made about the applicability of our theory to the valence electrons in sodium.

II. THE HIGH-DENSITY LIMIT

The partial annihilation rate $R(\mathbf{p})$, i.e., the transition probability per unit time for annihilation with emission of a photon pair of momentum $\mathbf{p}$, is given by[4]

$$R(\mathbf{p})=\frac{\lambda(-i)^2}{V}\int d^3\mathbf{x}d^3\mathbf{y}\, e^{-i\mathbf{p}\cdot(\mathbf{x}-\mathbf{y})} \times G_{ep}(\mathbf{x}t,\mathbf{x}t;\,\mathbf{y}t^+,\mathbf{y}t^+), \quad (2.1)$$

where the notation is as given in K-II, except for the constant $\lambda=\lambda_0(1/n_0)$. The quantities $4\lambda_0$ and n_0 are, respectively, the total annihilation rate and the electron density at the positron in singlet positronium. Denote by $u(\mathbf{k};\omega)$ the Fourier transform of the effective potential which is defined as the sum of all the simplest polarization diagrams, i.e., the repeated bubbles. If this effective force is introduced into the first-order ladder graph, its contribution to $R(\mathbf{p})$ is

$$R^{\text{h.d.}}(\mathbf{p})=\frac{i\lambda}{V^2}\sum_{\mathbf{kq}}\int\frac{d\omega d\epsilon d\epsilon'}{(2\pi)^3}G_e^0(\mathbf{k}+\mathbf{q};\omega+\epsilon)G_e^0(\mathbf{q};\epsilon) \times u(\mathbf{k};\omega)G_p^0(\mathbf{p}-\mathbf{q}-\mathbf{k};\epsilon'-\omega)G_p^0(\mathbf{p}-\mathbf{q};\epsilon'). \quad (2.2)$$

By a series of algebraic steps almost identical to those described in Sec. III of K-II, expression (2.2) can be reduced to

$$R^{\text{h.d.}}(\mathbf{p})=\frac{2i\lambda}{V^2}\sum_{\mathbf{k}}\int_{-\infty}^{+\infty}\frac{d\omega}{2\pi}\frac{u(\mathbf{k};\omega)}{k^2-\omega-i0^+} \times\left[\frac{\theta(|\mathbf{p}-\mathbf{k}|-p_F)\theta(p_F-p)}{\mathbf{p}^2-(\mathbf{p}-\mathbf{k})^2-\omega+i0^+} -\frac{\theta(p_F-|\mathbf{p}-\mathbf{k}|)\theta(p-p_F)}{\mathbf{p}^2-(\mathbf{p}-\mathbf{k})^2-\omega-i0^+}\right], \quad (2.3)$$

where $\theta(k-p_F)$ is the usual theta function equal to 1 for $k>p_F$ and zero otherwise. From (2.3), it is clear that $R^{\text{h.d.}}(\mathbf{p})$ is nonzero for both $p>p_F$ and $p<p_F$. This fact was overlooked in K-II where the entire contribution was assigned to the range $p<p_F$.

In the remainder of this section we will be concerned only with the case $p<p_F$, i.e., the first term of (2.3). As written in the limit of an infinite crystal, $R^{\text{h.d.}}(\mathbf{p})$ is given by a fourfold integral, which can be reduced to a double integral by standard techniques. This integral must then be evaluated on a computer. We need not reproduce the details here.[5] The numerical results for $r_s=3.79$ are shown in Fig. 1. The variation with momentum of the enhancement factor $\epsilon^{\text{h.d.}}(\mathbf{p})$ defined by $R^{\text{h.d.}}(\mathbf{p})=(\lambda/V)\epsilon^{\text{h.d.}}(\mathbf{p})$ is quite large. Its value at $p=0.9p_F$ is 22% larger than at $p=0.1p_F$. It is relevant to compare this enhancement factor with that obtained from (2.3) when the dynamic effective potential is replaced by its static limit $u(\mathbf{k};\omega=0)$. Note that in this case the contribution for $p>p_F$ vanishes. Denote the contribution for $p<p_F$ by $R^{\text{s.l.}}(\mathbf{p})=(\lambda/V)\epsilon^{\text{s.l.}}(\mathbf{p})$. If a plasmon correction is introduced,[6] $\epsilon^{\text{s.l.}}(\mathbf{p})$ agrees well with $\epsilon^{\text{h.d.}}(\mathbf{p})$ around $p=0$ but as p approaches p_F, $\epsilon^{\text{h.d.}}(\mathbf{p})$ increases much more rapidly. Thus, replacing the dynamic potential by its static limit in the first-order ladder graph tends to underestimate the variation across the electron sea of the corresponding enhancement factor. At first sight this may be disturbing, since the largest concentration of electrons is around the Fermi surface and since it is the static potential which is used in K-II to extend the theory to include higher order ladder graphs. However, it is only after self-energy effects are introduced into the analysis that the true value of such an approximation can be appreciated.

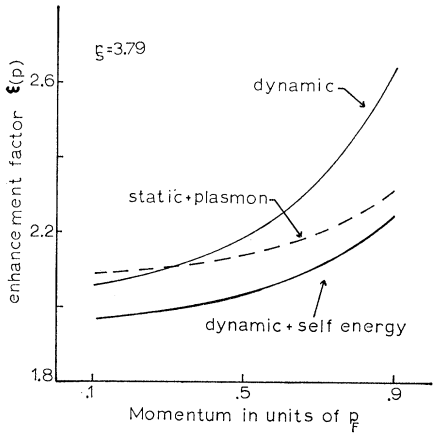

FIG. 1. The variation with momentum of the enhancement factor $\epsilon(\mathbf{p})$ for various cases. The fast-rising solid curve gives $\epsilon^{\text{h.d.}}(\mathbf{p})$ coming from the first-order ladder graph with full dynamic effective potential included. The lower solid curve is $\epsilon^{\text{h.d.}}(\mathbf{p})$ corrected for both electron and positron self-energies. The dashed curve is $\epsilon^{\text{s.l.}}(\mathbf{p})$ corrected for the plasmon, where $\epsilon^{\text{s.l.}}(\mathbf{p})$ stands for $\epsilon^{\text{h.d.}}(\mathbf{p})$ with the dynamic effective potential replaced by its static limit. These curves are all for $\alpha=0.2$. The parameter α is related to r_s by $\alpha=r_s/(1.919\pi^2)$.

III. SELF-ENERGY EFFECTS FOR $p<p_F$

Besides the ladder graph, there are two pure self-energy diagrams occurring in first-order perturbation

[4] This formula is given by R. A. Ferrell, Rev. Mod. Phys. **28**, 308 (1956). Also if $R(p)$ is summed over all momenta p we recover Eq. (3) of Ref. 1, to within a proportionality constant.

[5] The detailed manipulations involved, as well as a discussion of the numerical work, can be found in J. P. Carbotte, Ph.D. Thesis, McGill University, 1964 (unpublished).

[6] For a discussion of the meaning of this plasmon correction see Ref. 1, Sec. IV.

theory. They are shown in Fig. 2 and are the first-order terms in the expansion of the self-energy product $G_e(x_1;x_1')G_p(x_2;x_2')$.[7] The contribution to $R(\mathbf{p})$ from such a product can be written as

$$R(\mathbf{p})=\frac{\lambda}{V}\sum_{\mathbf{k}}P_e(\mathbf{p}-\mathbf{k})P_p(\mathbf{k}), \tag{3.1}$$

where $P_e(\mathbf{k})$ and $P_p(\mathbf{k})$ are, respectively, the electron and positron probability of occupation of a state of momentum $\mathbf{k}$. That is,

$$P_e(\mathbf{k})=i\int\frac{d\omega}{2\pi}G_e(\mathbf{k};\omega)e^{i\omega 0^+}=\langle|a_{\mathbf{k}}^\dagger a_{\mathbf{k}}|\rangle \tag{3.2a}$$

and

$$P_p(\mathbf{k})=i\int\frac{d\omega}{2\pi}G_p(\mathbf{k}\cdot\omega)e^{i\omega 0^+}=\langle|b_{\mathbf{k}}^\dagger b_{\mathbf{k}}|\rangle, \tag{3.2b}$$

where $a_{\mathbf{k}}^\dagger(b_{\mathbf{k}}^\dagger)$ is an operator which creates an electron (positron) in a state of momentum $\mathbf{k}$. The expectation values in (3.2) are to be taken in the fully interacting ground state for the system of electrons and positron. For the noninteracting system the positron function $P_p(\mathbf{k})$, for example, is $\theta(-k)$; i.e., it is equal to zero unless $\mathbf{k}=0$ in which case it is 1. This is simply a statement that the positron is thermalized on annihilation.[8]

Denote the contribution to the annihilation rate from the electron self-energy diagram 2(a) by $R^{\text{e.s.e.}}(\mathbf{p})$. Using the dynamic potential $u(\mathbf{q};\omega)$ instead of the bare Coulomb force $v(\mathbf{q})$, $R^{\text{e.s.e.}}(\mathbf{p})$ can be written as

$$R^{\text{e.s.e.}}(\mathbf{p})=\lambda/VP_e^{(1)}(\mathbf{p}), \tag{3.3}$$

with

$$P_e^{(1)}(\mathbf{p})=i\int\frac{d\omega}{2\pi}\frac{i}{V}\sum_{\mathbf{q}}\int\frac{d\epsilon}{2\pi}u(\mathbf{q};\epsilon)\times(G_e^0(\mathbf{p};\omega))^2G_e^0(\mathbf{p}-\mathbf{q};\omega-\epsilon). \tag{3.4}$$

It is a trivial matter to do the ω integration in (3.4) by contour integration in the complex ω plane. This leads to two distinct terms. The first term contributes only for $p<p_F$. It is negative and represents the first-order decrease in the probability of finding an electron in a state below the Fermi surface due to its interaction with the surrounding medium. On the other hand, the second term is nonvanishing only for $p>p_F$. It is positive and gives the first-order probability of finding an electron in a momentum state above the Fermi sea. The function $P_e^{(1)}(\mathbf{p})$ given by (3.4) is actually known, and it has been evaluated numerically by Daniel and Vosko.[9] We have redone the calculation and our results are presented in Fig. 3 for $r_s=3.79$. Note that in this figure we chose

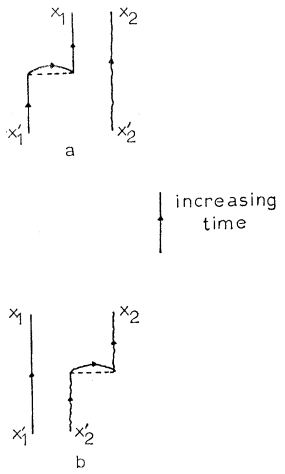

FIG. 2. The solid wavy line in diagram (a) represents the free propagation of a positron from x_2' to x_2 and stands for $G_p^0[x_2;x_2']$. Similarly the solid straight line in (b) describes the free propagation of an electron from x_1' to x_1 and stands for $G_e^0[x_1;x_1']$. The electron part of (a) is the first-order electron self-energy correction to the free-electron Green's function while the positron part of (b) is a similar positron self-energy correction.

to plot $\tilde{P}_e^{(1)}(\mathbf{p})\equiv\theta(p_F-p)+P_e^{(1)}(\mathbf{p})$ rather than $P_e^{(1)}(\mathbf{p})$. The main features of this curve are the discontinuity at $p=p_F$ and the tails beyond $p=p_F$ extending roughly to $p=1.5p_F$. For the moment let us ignore questions of convergence of the total perturbation series for $P_e(\mathbf{p})$ and assume that Fig. 3 is a reasonable approximation to the true momentum distribution. Since $P_e^{(1)}(\mathbf{p})$ is small at $\mathbf{p}=0$ but increases significantly as $\mathbf{p}$ tends towards p_F, making this correction to the "dynamic enhancement factor" $\epsilon^{\text{h.d.}}(\mathbf{p})$ (for $p<p_F$) will tend to smooth out its variation across the electron sea. The positron self-energy diagram 2(b) has much the same effect. Using an obvious notation, we have

$$R^{\text{p.s.e.}}(\mathbf{p})=\frac{\lambda}{V}\sum_{\mathbf{k}}\theta(p_F-|\mathbf{p}-\mathbf{k}|)P_p^{(1)}(\mathbf{k}), \tag{3.5}$$

where $P_p^{(1)}(\mathbf{k})$ is the first-order correction to the positron occupation probability and is given by (3.4) with all three-electron free propagators appearing to be replaced by positron Green's functions. Doing the

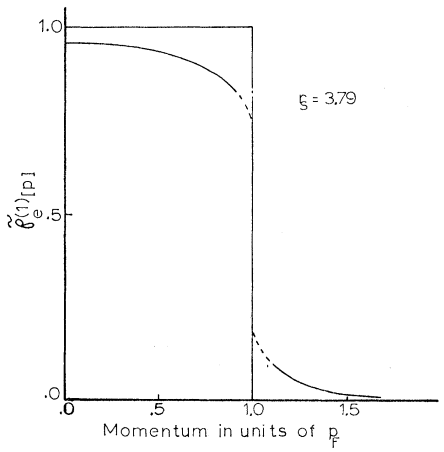

FIG. 3. The electron occupation probability to first order in perturbation theory for $r_s=3.79$.

[7] The positron self-energy graph 2(b) is zero as it stands. It is nevertheless convenient to consider such a diagram since it does contribute when the bare Coulomb line in it is replaced by some more appropriate effective potential.

[8] G. E. Lee-Whiting, Phys. Rev. **97**, 1557 (1955).

[9] E. Daniel and S. H. Vosko, Phys. Rev. **120**, 2041 (1960).

ω integration gives

$$P_p^{(1)}(\mathbf{k}) = -\theta(-k)\frac{i^3}{V}\sum_{\mathbf{q}}\int\frac{d\epsilon}{2\pi}u(\mathbf{q};\epsilon)\frac{-\theta(|\mathbf{k}-\mathbf{q}|)}{[-(\mathbf{k}-\mathbf{q})^2-\epsilon+i0^+]^2} + \theta(k)\frac{i^3}{V}\sum_{\mathbf{q}}\int\frac{d\epsilon}{2\pi}u(\mathbf{q};\epsilon)\frac{-\theta(-|\mathbf{k}-\mathbf{q}|)}{[\mathbf{k}^2-\epsilon-i0^+]^2}. \quad (3.6)$$

The first term in (3.6) contributes only for $\mathbf{k}=0$, while the second term is nonzero only for $\mathbf{k}\neq 0$. Thus

$$R^{\text{p.s.e.}}(\mathbf{p}) = \frac{\lambda}{V}\theta(p_F-p)P_p^{(1)}(\mathbf{k}=0) + \frac{\lambda}{V}\sum_{\mathbf{k}\neq 0}\theta(p_F-|\mathbf{p}-\mathbf{k}|)P_p^{(1)}(\mathbf{k}\neq 0). \quad (3.7)$$

The physical interpretation of (3.7) is straightforward. The first term is just the Sommerfeld partial annihilation rate multiplied by the first-order decrease in the positron occupation probability of a state of momentum $\mathbf{k}=0$. This is a negative contribution and is nonzero only for $p<p_F$. The second term contributes for arbitrary $\mathbf{p}$. It represents the free sampling of an unperturbed Fermi sea by a nonthermalized positron in a state of momentum $\mathbf{k}\neq 0$ weighted by the probability of finding the positron in the state $|\mathbf{k}\neq 0\rangle$ and summed over all such momenta $\mathbf{k}\neq 0$. For details see Ref. 5. The net effect of this correction on $\epsilon^{\text{h.d.}}(\mathbf{p})$ for $p<p_F$ is again to reduce its variation with momentum. The enhancement factor $\epsilon^{\text{h.d.}}(\mathbf{p})$ corrected for both electron and positron self-energies is plotted in Fig. 1. Clearly $\epsilon^{\text{s.l.}}(\mathbf{p})$ is a much better approximation to $\epsilon^{\text{h.d.}}(\mathbf{p})$ corrected for self-energies than to $\epsilon^{\text{h.d.}}(\mathbf{p})$ alone. More precisely, averaging $\epsilon^{\text{s.l.}}(\mathbf{p})+\epsilon^{\text{plasmon}}$ over the electron sea gives $2.25R^0$ as its contribution to the total annihilation rate (where R^0 is the Sommerfeld annihilation rate), while a similar average of $\epsilon^{\text{h.d.}}(\mathbf{p})$ and $\epsilon^{\text{h.d.}}(\mathbf{p})$ plus self-energy corrections contribute respectively $2.46R^0$ and $2.19R^0$. Thus, the enhancement factors given in K-II, which were computed using the static limit of the effective potential, can be thought of as already including to a large extent self-energy effects.

At this point we could proceed with a discussion of self-energy processes, investigating how they can be incorporated in a general calculation when the ladder graphs are considered to all orders and extending the theory to the case $p>p_F$. At the risk of making the discussion appear disjoint we prefer to leave these questions to later sections. For the moment it is convenient to turn to a discussion of some of the simpler second-order graphs.

IV. PARTICLE-HOLE INTERACTIONS

Before proceeding with the study of the second-order corrections to the ladder approximation for the electron-positron Green's function, it is perhaps useful to list and group them. First there are the second-order terms in the expansion of the product $G_e(x_1;x_1')G_p(x_2;x_2')$. These are pure self-energy diagrams and are disconnected. Next there are graphs describing one self-energy process, with a further electron-positron interaction line which connects the electron to the positron part. These graphs are obviously relevant to a discussion of how self-energy effects are to be included in the general scheme of summing ladder graphs to all orders. Finally, there are the two particle-hole interaction diagrams shown in Fig. 4. Graphs containing a polarization part have not been mentioned explicitly. They can be ignored if the Coulomb potential function $v(\mathbf{q})$ is replaced everywhere by the dynamic effective potential $u(\mathbf{q};\omega)$ or at least by its static limit.

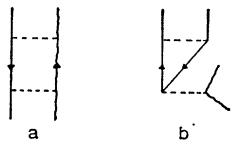

FIG. 4. The two second-order particle-hole interaction graphs. Diagram (a) represents a process in which there is a positron-electron hole interaction, while (b) describes an electron-electron hole interaction.

The two particle-hole interaction graphs will be the topic of this section. Begin by considering diagram 4(a). For definiteness, assume some specific time ordering for the various external lines as shown in Fig. 5. This represents a process in which there is a positron-electron hole interaction. More specifically, in the second scattering process the excited positron interacts with the electron hole in the Fermi sea. This is to be contrasted with the second-order ladder diagram, in which case the positron simply scatters a second time off the excited electron. Since the phase space available as final states to the doubly scattered electron is much larger than the corresponding phase space available to the scattered electron hole, it can be expected that the contribution to $R(\mathbf{p})$ from electron hole-positron interactions will be smaller than that from the ladder graph. Further, these contributions carry opposite signs. An electron-positron interaction is attractive and so increases the electron density at the positron, while an electron hole-positron correlation is repulsive, thus decreasing the annihilation rate.

Denote the contribution to the annihilation rate from diagram 4(a) by $R^{\text{p.-e.h.}}(\mathbf{p})$. It can be written as

$$R^{\text{p.-e.h.}}(\mathbf{p}) = \frac{\lambda}{V^3}\sum_{\mathbf{q}\mathbf{q}'\mathbf{k}}\int\frac{dv}{2\pi}u(\mathbf{q};0)u(\mathbf{q}';0)I(\mathbf{k}+\mathbf{q}';\mathbf{p}-\mathbf{k}+\mathbf{q};v) \times I(\mathbf{k};\mathbf{p}-\mathbf{k}+\mathbf{q}-\mathbf{q}';v)I(\mathbf{k}-\mathbf{q};\mathbf{p}-\mathbf{k}-\mathbf{q}';v), \quad (4.1)$$

where by definition,

$$I(\mathbf{l};\mathbf{l}';v) = \int\frac{d\epsilon}{2\pi}G_p^0(\mathbf{l};\epsilon)G_e^0(\mathbf{l}';\epsilon+v) = i\left[\frac{\theta(l)\theta(p_F-l')}{(l')^2-l^2-v+i0^+}-\frac{\theta(-l)\theta(l'-p_F)}{(l')^2-v-i0^+}\right]. \quad (4.2)$$

Note that in (4.1) the Coulomb potential $v(\mathbf{q})$ has been replaced by $u(\mathbf{q};0)$. Performing the v integration and the $\mathbf{k}$ summation in (4.1) and ignoring terms of order $1/V$, $R^{\text{p.-e.h.}}(\mathbf{p})$ can be rewritten as

$$R^{\text{p.-e.h.}}(\mathbf{p})=-\frac{\lambda}{V^3}\sum_{\mathbf{q}\mathbf{q}'}u(\mathbf{q};0)u(\mathbf{q}';0)\Bigg[2\frac{\theta(|\mathbf{q}+\mathbf{q}'|)\theta(p_F-p)\theta(q)\theta(p_F-|\mathbf{p}-\mathbf{q}'|)\theta(|\mathbf{p}-\mathbf{q}-\mathbf{q}'|-p_F)}{[p^2-(\mathbf{q}+\mathbf{q}')^2-(\mathbf{p}-\mathbf{q}-\mathbf{q}')^2][(\mathbf{p}-\mathbf{q}')^2-\mathbf{q}^2-(\mathbf{p}-\mathbf{q}-\mathbf{q}')^2]}$$
$$+\frac{\theta(q')\theta(p_F-|\mathbf{p}+\mathbf{q}|)\theta(|\mathbf{p}+\mathbf{q}-\mathbf{q}'|-p_F)\theta(q)\theta(p_F-|\mathbf{p}-\mathbf{q}'|)}{[(\mathbf{p}+\mathbf{q})^2-(q')^2-(\mathbf{p}+\mathbf{q}-\mathbf{q}')^2][(\mathbf{p}-\mathbf{q}')^2-q^2-(\mathbf{p}+\mathbf{q}-\mathbf{q}')^2]}\Bigg]. \quad (4.3)$$

The first term in (4.3) contributes only for $p<p_F$, while the second is nonzero for arbitrary momentum $\mathbf{p}$. Such contributions are exactly of the type that would occur in a "time-independent perturbation theory" formalism. It is easy to construct individual diagrams for such terms which can then be interpreted directly in terms of initial and final states for the electron system. The simplest quantitative estimate of (4.3) that can be made is in the limit $\mathbf{p}=0$. In this case we have

$$R^{\text{p.-e.h.}}(\mathbf{p})=-\frac{\lambda}{V^3}\sum_{\mathbf{q}\mathbf{q}'}u(\mathbf{q};0)u(\mathbf{q}';0)$$
$$\times\Bigg[\frac{2\theta(p_F-q')\theta(|\mathbf{q}+\mathbf{q}'|-p_F)}{[-2[\mathbf{q}+\mathbf{q}']^2][(q')^2-q^2+(\mathbf{q}+\mathbf{q}')^2]}$$
$$+\frac{\theta(p_F-q)\theta(|\mathbf{q}+\mathbf{q}'|-p_F)\theta(p_F-q')}{[q^2-(q')^2+(\mathbf{q}+\mathbf{q}')^2][(q')^2-q^2-(\mathbf{q}+\mathbf{q}')^2]}\Bigg]. \quad (4.4)$$

In (4.4) change all summations to integrations, measure all momenta in units of the Fermi momentum p_F and introduce the parameter $\alpha=r_s/(1.919\pi^2)$. The resulting expression can be written as

$$R^{\text{p.-e.h.}}(\mathbf{p})=\frac{\lambda}{V}(I_1+I_2),$$

with

$$I_1=-\alpha^2\int_{\substack{|\mathbf{q}+\mathbf{q}'|>1\\ q'<1}}d^3\mathbf{q}d^3\mathbf{q}'U(\mathbf{q})U(\mathbf{q}')$$
$$\times\frac{1}{(\mathbf{q}+\mathbf{q}')^2[(\mathbf{q}+\mathbf{q}')^2+q^2-(q')^2]} \quad (4.5)$$

and

$$I_2=-\alpha^2\int_{\substack{|\mathbf{q}+\mathbf{q}'|>1\\ q<1,\ q'<1}}d^3\mathbf{q}d^3\mathbf{q}'U(\mathbf{q})U(\mathbf{q}')$$
$$\times\frac{1}{[(\mathbf{q}+\mathbf{q}')^2+(q')^2-q^2][(\mathbf{q}+\mathbf{q}')^2-(q')^2+q^2]}. \quad (4.6)$$

In integrals (4.5) and (4.6) the potential function $U(\mathbf{q})$ stands for

$$U(\mathbf{q})=1\Big/\left(q^2+2\pi\alpha\left[1-\frac{1}{2k}(1-\tfrac{1}{4}k^2)\ln\left(\frac{k-2}{k+2}\right)^2\right]\right). \quad (4.7)$$

If the momentum dependence of $R^{\text{p.-e.h.}}(\mathbf{p})$ is neglected, i.e., if it is approximated by $\theta(p_F-p)R^{\text{p.-e.h.}}(\mathbf{p}=0)$, its contribution $R^{\text{p.-e.h.}}$ to the total annihilation rate is given by $R^0(I_1+I_2)$. For the numerical evaluation of I_1 and I_2, see Ref. 5. The results are plotted in Fig. 6. For $\alpha=0.1$, $R^{\text{p.-e.h.}}$ reduces the annihilation rate by approximately 6% of R^0, while for $\alpha=0.2$ the reduction is 10% of R^0, which is quite substantial. However, as we shall see next, the electron hole-electron interaction diagram has approximately the opposite effect.

Our task now is to evaluate the contribution to $R(\mathbf{p})$ from diagram 4(b) which involves an electron-electron hole interaction process. We expect $R^{\text{e.-e.h.}}(\mathbf{p})$ to be positive and, from phase-space considerations, to be slightly smaller than $|R^{\text{p.-e.h.}}(\mathbf{p})|$. Proceeding in the same fashion as outlined for the positron-electron hole

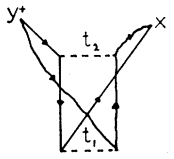

FIG. 5. A specific time ordering of graph 4(a).

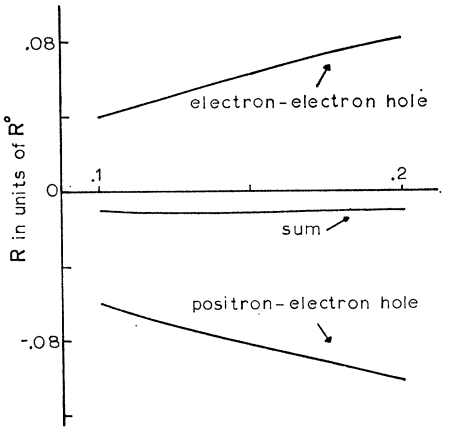

FIG. 6. Contribution to the total annihilation rate, in units of R^0, from positron- and electron-electron hole interaction processes. The sum of these two contributions amounts to a reduction of the total annihilation rate of about 2% of R^0 (for any α).

correlation term we obtain

$$R^{\text{e.}-\text{e.h.}}(\mathbf{p})=\frac{\lambda(-i)^2}{V^3}\sum_{\mathbf{q}\mathbf{q}'}u(\mathbf{q};0)u(\mathbf{q}';0)\cdot 2\theta(q)\Bigg[-\frac{\theta(|\mathbf{p}+\mathbf{q}|-p_F)\theta(p_F-p)\theta(|\mathbf{p}-\mathbf{q}'+\mathbf{q}|-p_F)\theta(p_F-|\mathbf{p}-\mathbf{q}'|)}{[p^2-(\mathbf{p}+\mathbf{q})^2-q^2][(\mathbf{p}-\mathbf{q}')^2-(\mathbf{p}+\mathbf{q}-\mathbf{q}')^2-q^2]}$$
$$+\frac{\theta(|\mathbf{p}+\mathbf{q}|-p_F)\theta(p_F-p)\theta(p_F-|\mathbf{p}+\mathbf{q}-\mathbf{q}'|)\theta(|\mathbf{p}-\mathbf{q}'|-p_F)}{[-q^2+p^2-(\mathbf{q}+\mathbf{p})^2][(\mathbf{p}-\mathbf{q}')^2-(\mathbf{p}+\mathbf{q}-\mathbf{q}')^2-p^2+(\mathbf{p}+\mathbf{q})^2]}$$
$$+\frac{\theta(p_F-|\mathbf{p}+\mathbf{q}|)\theta(p-p_F)\theta(|\mathbf{p}-\mathbf{q}'+\mathbf{q}|-p_F)\theta(p_F-|\mathbf{p}-\mathbf{q}'|)}{[-q^2+(\mathbf{p}-\mathbf{q}')^2-(\mathbf{p}-\mathbf{q}'+\mathbf{q})^2][p^2-(\mathbf{p}+\mathbf{q})^2-(\mathbf{p}-\mathbf{q}')^2+(\mathbf{p}-\mathbf{q}'+\mathbf{q})^2]}\Bigg]. \quad (4.8)$$

The first two terms are nonzero only if $p<p_F$, while the third vanishes unless $p>p_F$. To get an idea of the magnitude of (4.8), again take the case $\mathbf{p}=0$. In this limit $R^{\text{e.}-\text{e.h.}}(\mathbf{p})$ can be written as

$$R^{\text{e.}-\text{e.h.}}(\mathbf{p}=0)=(\lambda/V)(J_1+J_2),$$

with

$$J_1=\alpha^2\int_{\substack{|\mathbf{q}+\mathbf{q}'|\leq 1\\ q>1,\ q'<1}}d^3\mathbf{q}d^3\mathbf{q}'U(\mathbf{q})U(\mathbf{q}')\times\frac{1}{q^2[q^2-(q')^2+(\mathbf{q}+\mathbf{q}')^2]} \quad (4.9)$$

and

$$J_2=\alpha^2\int_{\substack{|\mathbf{q}+\mathbf{q}'|\leq 1\\ q>1,\ q'>1}}d^3\mathbf{q}d^3\mathbf{q}'U(\mathbf{q})U(\mathbf{q}')\times\frac{1}{q^2[(q')^2+q^2-(\mathbf{q}+\mathbf{q}')^2]}. \quad (4.10)$$

In Fig. 6 we have plotted $R^{\text{e.}-\text{e.h.}}\equiv\sum_{\mathbf{p}}\theta(p_F-p)\times R^{\text{e.}-\text{e.h.}}(\mathbf{p}=0)$; it cancels against $R^{\text{p.}-\text{e.h.}}$. As expected, the sum of these two effects still amounts to a reduction of the annihilation rate, but only by approximately 2% of R^0, there being very little variation with valence electron density.

At this point we would like to emphasize that in our investigation of particle-hole correlations no enhancement effects have been accounted for. Once the electron-positron pair is excited, we have considered the possibility of either a positron or an electron correlation with the electron hole left behind in the passive electron sea. But then the excited pair annihilates without any direct interaction between them. To account for such a direct interaction, higher order diagrams consisting of a particle-hole interaction part and a further series of ladder processes would have to be included. Two examples of the diagrams we have in mind are shown in Fig. 7, for the case of a positron-electron hole correlation. From the work in K-II, it can be expected that these enhancement effects are very important. But in view of the cancellation found between electron hole-electron and -positron interactions, it is not worthwhile to pursue the calculation further since this cancellation must remain to all orders. A similar cancellation will be discussed in detail in the next two sections.

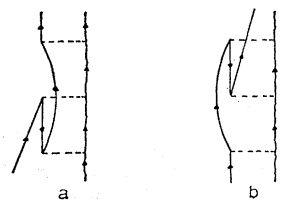

FIG. 7. Two diagrams describing a positron-electron hole interaction and a further direct correlation between the annihilating pair.

V. ANNIHILATION WITH EMISSION OF MOMENTUM $p>p_F$

As a first step in generalizing the theory of the previous sections to include events with release of momentum $p>p_F$, it is natural to begin by determining the tails expected in the two-photon counting rate when the positron force is ignored. In this instance the electron-positron Green's function reduces to $G_e(x_1;x_1')\times G_p{}^0(x_2;x_2')$ and from (3.1) we have

$$R(\mathbf{p})=\frac{\lambda}{V}\sum_{\mathbf{k}}P_e(\mathbf{p}-\mathbf{k})\theta(-k)=\frac{\lambda}{V}P_e(\mathbf{p}). \quad (5.1)$$

The partial annihilation rate is directly proportional to the electron momentum distribution $P_e(\mathbf{p})$. The quantity that is measured in the usual angular correlation experiment, however, is not $R(\mathbf{p})$ but rather $\sum_{p_xp_y}R(\mathbf{p})$, where the z direction is determined by the geometry of the experimental setup. The two-photon counting rate $\bar{R}(p_F\gamma_3)$, in units of $\frac{3}{4}R^0$, is given by $\int_{\gamma_3}^{\infty}\gamma d\gamma P(p_F\gamma)$, where γ_3 is momentum along the z direction measured in units of p_F.

The counting rate corresponding to the momentum distribution of Fig. 3 is plotted in Fig. 8(a). Note the short but rather broad tails in this curve and the discontinuity in slope at $\gamma_3=1$. Since it is now possible to differentiate the experimental data, it is usually the derivative rather than the counting rate itself which is plotted. For the convenience of the reader this quantity is shown in Fig. 8(b). It is observed that the discontinuity in this last curve at $\gamma_3=1$ is just the discontinuity at the Fermi surface in the electron momentum distribution. Also, should this simple model be valid, present day experiments are more than adequate to discriminate between a simple Sommerfeld momentum distribution and that of Fig. 3.

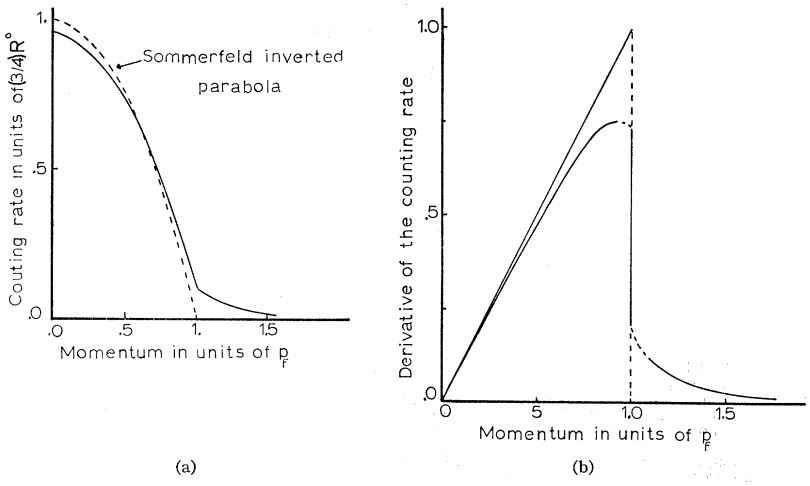

FIG. 8. (a) The two-photon counting rate corresponding to the electron momentum distribution given in Fig. 3 and determined under the assumption that the positron Coulomb field can be neglected. (b) The derivative of the two-photon counting rate plotted in (a).

The results so far are based on a first-order calculation for the electron momentum distribution. The question arises of how good a representation this is of the real momentum distribution. Two papers are particularly relevant to this point. The first is some work by Luttinger[10] in which he shows that the discontinuity at $p=p_F$ remains to all orders in the electron-electron repulsion, even in the case when the crystal periodic field is included. Second, the very recent work by Geldart, Houghton, and Vosko[11] is even more pertinent. They show that, in general, approximating directly to the electron Green's function $G_e(x;x')$ to get the probability of occupation function $P_e(\mathbf{p})$ leads to a poorly convergent series. They find that it is much better to introduce from the beginning the irreducible self-energy operator $M(x;x')$.[12] In such a formulation the Green's function is thought of as a functional of M and it is the irreducible self-energy operator which is ultimately approximated to, in order to get concrete results. Only in this way can one hope to get reasonable values for $P_e(\mathbf{p})$. It is very difficult to carry through such a program; indeed, Geldart *et al.* restrict themselves to a calculation of the discontinuity in $P_e(\mathbf{p})$ at $p=p_F$. The point we wish to make here is that this more careful treatment leads to results which agree quite well with the discontinuity arrived at from our rather naive approach. Further, $P_e(\mathbf{p})$ must satisfy the rigid sum rule that $\sum_{\mathbf{p}} P_e(\mathbf{p})$ should be equal to the valence electron density. Because of these rather stringent conditions it is hard to see how the true momentum distributlon could be very different from that of Fig. 3 which must be qualitatively, if not quantitatively, correct. This is particularly sensible in view of the fact that the entire series for the momentum distribution is at best an asymptotic series and should not be carried too far. In any case, we are not so much interested here in the pure electron gas part of the perturbation series as in the modifications introduced into the problem by the existence of the positron force. Thus we simply assume that Fig. 3 is a reasonable approximation to $P_e(\mathbf{p})$ and neglect all further pure electron self-energy diagrams. At worst, our calculation can be thought of as a model calculation.

In the remainder of this section we will be concerned only with the modifications in the two-photon counting rate introduced by the positron Coulomb field. The simplest such correction comes from the positron self-energy diagram 2(b). An expression for this quantity has been given in Sec. III. Its numerical evaluation shows that positron self-energies roughly double the tails in the angular correlation curve coming from electron self-energies.

Self-energy effects are however only part of the complete picture. We have emphasized in Sec. II that the first-order ladder graph with full dynamic effective potential includes contributions to $R(\mathbf{p})$ for $p>p_F$, as well as for $p<p_F$. It was also pointed out that this result depends on the dynamic nature of the effective potential. A screened two body static force would give zero for $R^{\text{h.d.}}(\mathbf{p})$ with $p>p_F$. Consider Fig. 9 in which the first-order ladder graph is shown, with the effective potential expanded in its various polarization bubble

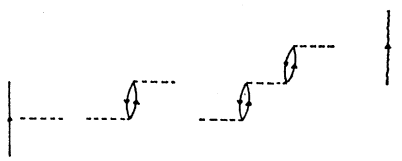

FIG. 9. The first-order ladder graph with full dynamic effective potential expanded in its constituent polarization bubbles. Since, for $p>p_F$, the first bare Coulomb step does not contribute to $R(\mathbf{p})$, the interaction process in this case is of a screened dipole character. For $p<p_F$ it is a screened monopole interaction occurring between the annihilating pair.

[10] J. M. Luttinger, in *The Fermi Surface*, edited by W. A. Harrison and M. B. Webb (John Wiley & Sons, Inc., New York, 1960), p. 2.

[11] D. J. W. Geldart, A. Houghton, S. H. Vosko, Can. J. Phys. 42, 1938 (1964).

[12] For a definition of the irreducible self-energy operator M see for instance Ref. 2.

TABLE I.[a] For momentum greater than the Fermi momentum, the sum $R^{\text{sum}}[p_F\gamma]$ of the contributions to the partial annihilation rate from the first-order ladder, electron- and positron-self-energy graphs with full dynamic effective potential included. The parameter $\alpha=0.2$.

Momentum γ in units of p_F	$R^{\text{e.s.e.}}[p_F\gamma]$	$R^{\text{p.s.e.}}[p_F\gamma]$	$R^{\text{h.d.}}[p_F\gamma]$	$R^{\text{sum}}[p_F\gamma]$
1.1	0.1021	0.1107	−0.2037	0.0075
1.3	0.0359	0.0456	−0.0776	0.0030
1.5	0.0156	0.0199	−0.0344	0.0014
1.7	0.0067	0.0091	−0.0156	0.0007
1.9	0.0031	0.0041	−0.0073	0.0003

[a] Note that in this table as well as in Table II we have suppressed, for clarity, a factor λ/V which should multiply each of the entries. The first three columns in this table are given for the convenience of the reader so that he can see the extent of the cancellation mentioned in the text. It should be noted however, that each entry in the fourth column is *not* simply the sum of the first three numbers in that row. Because of the large cancellation, it was necessary to write a more accurate program evaluating the sum directly rather than each of the three individual terms independently. While in $R^{\text{sum}}[p_F\gamma]$ all figures are significant figures only the first three are reliable in the other numbers quoted.

contributions. For $p>p_F$ the first bare Coulomb step contributes nothing to $R^{\text{h.d.}}(\mathbf{p})$. Thus, in this case, diagram 9 describes a screened dipole interaction process with no direct coupling between the annihilating pair. This is to be contrasted with the situation for $p<p_F$. In this instance the process described is a screened monopole interaction between the electron-positron pair. Since the screening charge around an electron is of a repulsive character as far as the positron is concerned, $R^{\text{h.d.}}(\mathbf{p})$ for $p>p_F$ must be negative. From (2.3) we have that $R_>^{\text{h.d.}}(\mathbf{p})$ is

$$R_>^{\text{h.d.}}(\mathbf{p})=\frac{\lambda(-2i)}{V^2}\sum_{\mathbf{k}}\int\frac{d\omega}{2\pi}u(\mathbf{k};\omega)\times\frac{\theta(p_F-|\mathbf{p}-\mathbf{k}|)}{(k^2-\omega-i0^+)(p^2-(\mathbf{p}-\mathbf{k})^2-\omega-i0^+)}. \quad (5.2)$$

If this integral is reduced and evaluated numerically, one finds that it is of the same order of magnitude as the sum of $R_>^{\text{e.s.e.}}(\mathbf{p})$ and $R_>^{\text{p.s.e.}}(\mathbf{p})$ and thus cancels almost completely the tails expected from electron and positron self-energies combined. The detailed numerical results for the sum $R_>^{\text{h.d.}}(\mathbf{p})+R_>^{\text{e.s.e.}}(\mathbf{p})+R_>^{\text{p.s.e.}}(\mathbf{p})$ are given in Table I. The extent of the cancellation is remarkable. It is true that this result depends on our perhaps poor treatment of electron and positron self-energy processes. However, a more careful treatment of these effects cannot change the fact that a large cancellation must occur and that we cannot expect tails in the final photon counting rate at all comparable with those predicted on a naive model where the positron force field is ignored.

For completeness we now mention the effect on $R(\mathbf{p})$ for $p>p_F$ of the two particle-hole interaction graphs studied in Sec. IV. Both positron and electron-electron hole interaction graphs contribute. For $p>p_F$, $R_>^{\text{p.-e.h.}}(\mathbf{p})$ and $R_>^{\text{e.-e.h.}}(\mathbf{p})$ are given, respectively, by the second term of (4.3) and the third term of (4.8). These two integrals were evaluated by using a Monte Carlo integration method. The results for various values of momentum and electron gas densities are given in Table II. They are an order of magnitude smaller than the self-energy and polarization contributions. They also carry opposite signs, making such effects even less important.

VI. EXTENSION TO INCLUDE ENHANCEMENT FACTORS FOR $p>p_F$

We have not as yet considered enhancement effects. For instance, take the case of electron self-energies. Because of its interaction with the surrounding medium, there is a probability for an electron to be above the Fermi sea and then be annihilated with the zero momentum positron. But in this simple process the attractive force between the annihilating pair is not included. This attraction could increase considerably the electron density at the positron. To take account of this enhancement effect it is clear that we must sum, at least in some approximation, the entire set of ladder diagrams with self-energy effects included in the electron lines. The type of thing we would like is to write the contribution to $R(\mathbf{p})$ from all these ladder graphs in the form

$$R(p)=(\lambda/V)P_e(\mathbf{p})\epsilon(\mathbf{p}), \quad (6.1)$$

where $\epsilon(\mathbf{p})$ is an enhancement factor given by the square of some Bethe-Goldstone amplitude. This amplitude is to describe adequately the modification in the wave function of the annihilating pair due to their interaction once the electron is so to speak above the sea. It is not obvious *a priori* that the program just outlined can be carried out in detail. Physically, it seems reasonable, and should serve as a guide to the correct picture.

We shall not present the complete analysis but simply

TABLE II. The contributions to the partial annihilation rate, for momentum greater than the Fermi momentum, coming from the second order positron-electron hole and electron-electron hole interaction graphs.

Momentum γ in united of p_F	1.0	1.2	1.4	1.6	1.8	2.0	
$R^{\text{p.-e.h.}}[p_F\gamma]=$	−0.0038	−0.0031	−0.0017	−0.0010	−0.0006	−0.0003	$\alpha=0.1$
$R^{\text{e.-e.h.}}[p_F\gamma]=$	0.0130	0.0096	0.0045	0.0022	0.0011	0.0005	
$R^{\text{p.-e.h.}}[p_F\gamma]=$	−0.0065	−0.0041	−0.0022	−0.0019	−0.0010	−0.0006	$\alpha=0.2$
$R^{\text{p.-e.h.}}[p_F\gamma]=$	0.0226	0.0113	0.0058	0.0038	0.0020	0.0012	

state the results. Normally, we would like to treat the ladder diagrams containing self-energy insertions into all electron and positron lines as well as including the fully dynamic potential in each ladder step. In practice, we have limited ourselves to a linearized approximation, including any ladder diagram in which only one electron or positron line has been corrected for self-energies or alternatively a ladder step corrected for the dynamic nature of the polarization.

When a single-electron self-energy correction is made, the contribution to $R(\mathbf{p})$ is obtained as

$$R(\mathbf{p})=\frac{i\lambda}{V}\int\frac{dE}{2\pi}G_e(\mathbf{p};E)[\sum_{\mathrm{m}}\Omega^0{}_{\mathrm{m,p-m;p,0}}(E)]^2, \quad (6.2)$$

where the Bethe-Goldstone amplitude Ω^0 satisfies the equation[13]

$$\Omega^0{}_{\mathrm{m,n;}}(E)_{\mathrm{m',n'}}=\delta_{\mathrm{m,m'}}\delta_{\mathrm{n,n'}}+\frac{\theta(m-p_F)\theta(n)}{m^2+n^2-E-i0^+}\frac{1}{V}$$
$$\times\sum_{\mathbf{q}}u(\mathbf{q};0)\Omega^0{}_{\mathrm{m-q,n+q;m',n'}}(E). \quad (6.3)$$

Clearly (6.2) can be written in the form

$$R(\mathbf{p})=\frac{i\lambda}{V}\int\frac{dE}{2\pi}G_e(\mathbf{p};E)\epsilon(\mathbf{p};E), \quad (6.4)$$

where we have introduced a frequency-dependent enhancement factor

$$\epsilon(\mathbf{p};E)=[\sum_{\mathrm{m}}\Omega^0{}_{\mathrm{m,\,p-m;\,p,0}}(E)]^2. \quad (6.5)$$

Direct evaluation of the amplitude $\Omega^0(E)$ by solving numerically Eq. (6.3) shows that for E in the relevant range, i.e., near $p_F{}^2$, $\epsilon(p;E)$ is a slowly varying function of energy. Thus we fix E at some convenient value $\hat{E}$ and obtain from (6.4)

$$R(\mathbf{p})=(R_>{}^{\mathrm{e.s.e.}}(\mathbf{p}))\epsilon(\mathbf{p};\hat{E}), \quad (6.6)$$

which is an obvious generalization of (6.1).

Indeed, one obtains by including the positron self-energy ladder diagrams and the polarization ladder diagrams, all for $p>p_F$, a composite result

$$R(\mathbf{p})=(R_>{}^{\mathrm{e.s.e.}}(\mathbf{p})+R_>{}^{\mathrm{p.s.e.}}(\mathbf{p})$$
$$+R_>{}^{\mathrm{h.d.}}(\mathbf{p}))\epsilon(\mathbf{p};\hat{E}). \quad (6.7)$$

To be clearer the graphs on which (6.7) is based are shown in Fig. 10.

The enhancement factor $\epsilon(\mathbf{p};\hat{E})$ is of the same order of magnitude as that quoted in K-II for $p<p_F$. Thus, when the direct Coulomb coupling between the annihilating electron-positron pair is taken into account the tails coming from the sum of electron and positron self-energies, as well as polarization effects, are to be multiplied by roughly the same enhancement factor as is the central part of the distribution. But these tails are still quite negligible in relation to the central parabola because of the previously mentioned cancellation, and are not at all comparable to those coming from electron self-energies alone.

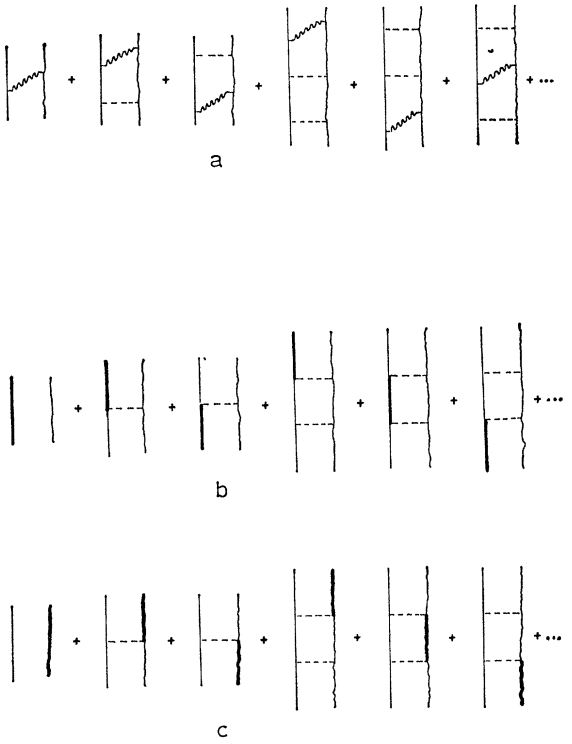

FIG. 10. The sum (a) of all ladder graphs with dynamic potential included in one and only one step in each order of perturbation theory. The sum (b) of all ladder graphs with electron self-energies included in one and only one of the electron lines in each order (all positron propagators are free propagators). The sum (c) is a similar sum including positron self-energies in one and only one line in each order.

VII. DISCUSSION AND CONCLUSIONS

By a careful, if somewhat tedious analysis we have managed to show that the enhancement factors given in K-II can be interpreted as already including the major part of the self-energy corrections to the ladder approximation. This comes about because of the fortunate circumstance that replacing the dynamic potential in the first-order ladder graph by its static limit has much the same effect on the corresponding enhancement factor as correcting it for self-energy processes. It is true that this result was obtained only for the case when the Born approximation is adequate to describe the electron-positron scattering process. However, by analogy with the work of Secs. V and VI it appears plausible that this result is more generally valid and applies even when higher order ladder graphs are considered.

[13] Except for the energy dependence E this equation is the same as that given in K-II.

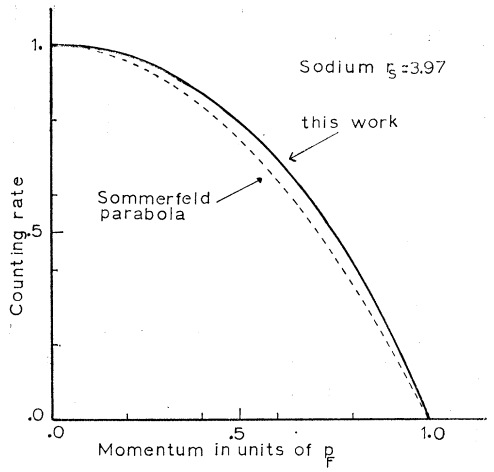

FIG. 11. The solid curve is the final result for the counting rate arrived at in this paper while the dashed curve is given for reference and is the Sommerfeld inverted parabola. The units on the vertical scale are vastly different for the two curves. For the Sommerfeld parabola the counting rate is in units of $\frac{3}{4}R^0$, so that the area under this curve simply gives a total rate of R^0, as it should. For the solid curve the units have been adjusted so as to normalize the counting rate at zero momentum to the Sommerfeld value: the appropriate units are $\frac{3}{4}R^0\times 13.46$.

Next we showed that although the two hole-particle interaction graphs can individually contribute roughly 10% to the total annihilation rate, they carry opposite signs and their sum amounts to no more than a 2% reduction. To this accuracy they can be ignored.

The question of tails entering the two-photon counting rate due to electron-electron repulsions was then investigated. Electron self-energies introduce a sufficient number of events with momentum $p>p_F$ to be experimentally detectable. This is also true of positron self-energies. However these two processes alone overlook an essential feature of the problem. The first-order ladder graph with full dynamic potential also contributes to $R(\mathbf{p})$ for $p>p_F$. This contribution is negative and quite large. It reduces the tails coming from electron and positron self-energies to the extent that they would be well below possible detection. Finally, this result was shown to hold even when the calculation is extended to include enhancement factors.

As a general conclusion we state that the positron force not only has a strong influence on the total rates as demonstrated in K-II, but also leads to subtle effects in the two-photon counting rate. That is, the counting rate of Fig. 8(a) which was computed under the assumption that the positron Coulomb field can be ignored bears little resemblance in detail to the curve predicted in this paper—essentially an inverted parabola bulging out slightly in the center as shown in Fig. 11, with no significant tails beyond p_F coming from electron-electron repulsions.

The theory developed in this paper applies to a particular metal only inasmuch as the detailed solid-state surroundings of the valence electrons can be ignored. For metallic sodium it is well known that in many instances the periodic crystal field can be neglected. It was shown by Carbotte[14] that this is indeed also the case for the positron-annihilation problem. By using an approach similar to that described in a paper by Berko and Plaskett,[15] it can be demonstrated that the lattice in sodium has little effect other than introducing core annihilation. It is true that there is a large number of high-momentum components present in the electron and positron Block states, but these enter with very small coefficients.

From a knowledge of the positron self-consistent Bloch state, core annihilation can be computed on a rigid-ion model. It is found to introduce broad and long tails in the angular correlation curve, and to contribute an amount of $1.02R^0$ to the total annihilation rate. These results were of course arrived at neglecting any direct electron-positron coupling. Since the core electrons are under the influence of a strong nuclear (or screened nuclear) field around which they can be considered to move, it is to be expected that enhancement factors for these electrons will be substantially smaller than those for the valence electrons. This is, in fact, consistent with both the experimental counting rate and the total annihilation rate. The prediction for the total annihilation rate made in K-II is 2.6×10^9 sec^{-1} while the experimental value given by Bell and Jørgensen[16] is 3.33×10^9 sec^{-1}. Assigning the difference entirely to core annihilation leads to a core enhancement factor of about 3.5. This is not inconsistent with the angular correlation curve given by Stewart.[17]

In the future we hope to return to the problem of core enhancement factors in sodium and thus be able to make a more careful comparison with experiment.

ACKNOWLEDGMENT

One of the authors (J. P. C.) would like to acknowledge the hospitality of the Laboratory of Atomic and Solid State Physics at Cornell University where the manuscript was prepared and where he was supported by the U. S. Office of Naval Research.

[14] See Ref. 5.
[15] S. Berko and J. S. Plaskett, Phys. Rev. **112**, 1877 (1958).
[16] R. E. Bell and M. H. Jørgensen, Can. J. Phys. **38**, 652 (1960).
[17] Perhaps the most convenient presentation of the data for our purpose is to be found in A. T. Stewart, J. B. Shand, J. J. Donaghy, and J. H. Kusmiss, Phys. Rev. **128**, 118 (1962).